Carbohydrate Polymers 80 (2010) 1062–1071

Contents lists available at ScienceDirect

Carbohydrate Polymers

journal homepage: www.elsevier.com/locate/carbpol

Chitosan oligosaccharides protect human umbilical vein endothelial cells from hydrogen peroxide-induced apoptosis

Hong-Tao Liu [a,b,c], Jun-Lin He [b], Wen-Ming Li [b], Zhu Yang [b], Ying-Xiong Wang [b], Xue-Fang Bai [a], Chao Yu [b,*], Yu-Guang Du [a,*]

[a] Dalian Institute of Chemical Physics, Chinese Academy of Sciences, Dalian 116023, China
[b] Institute for Life Sciences, Chongqing Medical University, Chongqing 400016, China
[c] The Graduate School of Chinese Academy of Sciences, Beijing 110864, China

ARTICLE INFO

Article history:
Received 11 October 2009
Received in revised form 7 January 2010
Accepted 11 January 2010
Available online 18 January 2010

Keywords:
Chitosan oligosaccharides
Hydrogen peroxide
Apoptosis
Human umbilical vein endothelial cell

ABSTRACT

This study aimed to investigate the protective effect of chitosan oligosaccharides (COS) on human umbilical vein endothelial cell (HUVEC) apoptosis induced by hydrogen peroxide (H_2O_2). We found that COS not only reversed the decrease of cell viability and proliferation activity, but ameliorated nuclear chromatin damage in H_2O_2-induced HUVECs. Additionally, COS contributed to the decrease of cytosolic Ca^{2+} level, increase of mitochondrial membrane potential, up-regulation of Bcl-2 mRNA, down-regulation of Bax mRNA, reduction of cleaved caspase-3 protein, inhibition of phosphorylated p38 mitogen-activated protein kinase (MAPK) and induction of phosphorylated Akt in HUVECs. Further, H_2O_2-induced caspase-3 activation could be suppressed by p38 MAPK inhibitor (SB203580) and up-regulated by phosphatidylinositol-3-kinase (PI3K) inhibitor (LY294002), indicating the involvement of p38 MAPK and PI3K/Akt signaling pathways. In conclusion, the results show that COS may effectively inhibit the H_2O_2-induced HUVEC apoptosis.

1. Introduction

Oxidative stress defined as excessive production of reactive oxygen species (ROS) has been involved in the pathogenesis of cardiovascular diseases such as atherosclerosis, hypertension, hypercholesteremia and diabetic vasculopathy (Cai, 2005). Generation of ROS causes oxidative damage to lipids, proteins, enzymes and may impair cellular functions, resulting in occurrence of apoptosis in severely damaged cells (Halliwell, 1997). As one of the most important ROS, hydrogen peroxide (H_2O_2) plays a central role in vascular pathophysiology (Griendling & FitzGerald, 2003). Several studies have evidenced that high concentration of H_2O_2 leads endothelial cells (ECs) to lose their membrane integrity and to undergo apoptosis (Irani, 2000). The underlying mechanisms of H_2O_2-induced EC apoptosis were partly characterized: (1) destruction of endogenous anti-oxidative defense systems in ECs (Luo & Xia, 2006); (2) involvement of apoptosis-related regulation signals such as Bcl-2 family and caspases, as well as mitogen-activated protein kinases (MAPKs) (Tuo, Wang, Yan, & Liao, 2004; Xu et al., 2008a, 2008b). Therefore, blockade of these pro-apoptotic pathways in ECs has been considered as an attractive therapeutic strategy to prevent or ameliorate the progression of vascular diseases induced by H_2O_2.

Chitosan is a cationic polysaccharide composed of β-1,4-linked 2-acetamido-D-glucose and β-1,4-linked 2-amino-D-glucose units with the latter usually exceeding 80% (Arvanitoyannis, Nakayama, & Aiba, 1998). Chitosan oligosaccharides (COS) are depolymerized products of chitosan by chemical and enzymatic hydrolysis. Traditionally, COS were widely used as functional materials for their biodegradability and adsorption properties (Du, Wang, Yuan, Wei, & Hu, 2009). In recent years, COS with different degree of polymerization (DP) and degree of deacetylation have been recommended as healthy food in Asian countries for various biological activities including anti-tumor, anti-hypertensive, anti-microbial and immunopotentiating activities (Nam, Kim, & Shon, 2007; Nishimura et al., 1984; Shon & Nam, 2005; Xu, Zhao, Han, & Du, 2007). COS also protect normal cells from apoptosis challenged by exogenous stimuli. For example, carboxymethyl-chitosan (39 kDa) was reported to inhibit interleukin-1β-induced apoptosis in rabbit chondrocytes (Chen, Liu, Du, Peng, & Sun, 2006), and apoptosis induced by serum starvation in human astrocytes could be suppressed by water-soluble chitosan (300 kDa, degree of deacetylation over 90%) (Koo et al., 2002). Moreover, COS (0.5–1 kDa, degree of deacetylation 90%) are known to exert good anti-oxidative activities in either cellular studies or cell-free assay (Je, Park, & Kim, 2004; Mendis, Kim, Rajapakse,

* Corresponding authors. Address: Laboratory of Natural products and Glyco-Engineering Research, Dalian Institute of Chemical Physics, CAS, 457, Zhong-shan Road, Dalian 116023, PR China. Tel.: +86 411 84379061; fax: +86 411 84379060.
E-mail addresses: yuchaom@163.com (C. Yu), articles1805@gmail.com (Y.-G. Du).

0144-8617/$ - see front matter © 2010 Elsevier Ltd. All rights reserved.
doi:10.1016/j.carbpol.2010.01.025

& Kim, 2007). In preliminary studies, we have proved that COS (<1 kDa, degree of deacetylation over 95%) attenuated H_2O_2-induced apoptosis in human umbilical vein endothelial cells (HUVECs) by repressing intracellular ROS and restoring damaged endogenous anti-oxidative enzymes (Liu et al., 2009). Nonetheless, it remains to be known what and how apoptosis-related regulation signals are implicated in the inhibitory effect of COS on EC apoptosis challenged by oxidative stress.

Considering the significance of EC apoptosis in pathogenesis of vascular diseases, this study was undertaken to evaluate the protective effect of COS on H_2O_2-induced apoptosis in HUVECs. We evaluated whether COS could attenuate the decrease in cell viability and proliferation of HUVECs induced by H_2O_2. Also, we assayed suppressive effect of COS on the damage of nuclear chromatin, loss of mitochondrial membrane potential and increase of Ca^{2+} influx in HUVECs. To further identify the potential mechanisms by which COS inhibited HUVEC apoptosis, we explored the roles of Bcl-2, Bax, caspase-3, p38 MAPK and phosphatidylinositol-3-kinase (PI3K)/Akt after H_2O_2 exposure.

2. Materials and methods

2.1. Chemicals and reagents

COS were prepared as previously described (degree of deacetylation over 95%) and endotoxin free by limulus amebocyte lysate test (Zhang, Du, Yu, Mitsutomi, & Aiba, 1999). The weight percentages of COS with DP 2–6 in oligomixture were 3.7%, 16.1%, 28.8%, 37.2% and 14.2%, respectively. 3-(4,5-Dimethylthiazol-2-yl)-2,5-diphenyltetrazolium bromide (MTT), H_2O_2 and 5,6-carboxyfluorescein diacetate succinimidyl ester (CFSE) were obtained from Sigma (St. Louis, MO, USA). Hoechst 33258 was purchased from Nanjing Key-Gen Biotech Co., Ltd. (Nanjing, China) and Tris-phenol from Bioer Technology Co., Ltd. (Hangzhou, China). MitoProbe™ JC-1 Assay Kit, fluo-3 AM and p38 MAPK inhibitor (SB203580) were obtained from Invitrogen Corporation (Carlsbad, CA, USA). Phosphatidylinositol 3-kinase (PI3K) inhibitor (LY294002) was purchased from Beyotime Institute of Biotechnology (Jiangsu, China). Rabbit anti-p38 MAPK, anti-phospho-p38 (p-p38) MAPK, anti-Akt, anti-phospho-Akt (p-Akt), anti-caspase-3 and anti-GAPDH polyclonal antibody, and horseradish peroxidase (HRP)-conjugated goat anti-rabbit IgG were obtained from Santa Cruz Biotechnology (Santa Cruz, CA, USA). Dulbecco's-modified Eagle's medium F12 (DMEM-F12) and fetal bovine serum (FBS) were purchased from Gibco (Grand Island, NY, USA).

2.2. Cell culture and drug treatment

HUVECs were isolated from normal human umbilical cords, digested with 0.05% trypsin and 0.02% EDTA, and eluted with DMEM-F12. Cells were cultured in DMEM-F12 supplemented with 10% FBS, 5 units/ml heparin, 30 μg/ml endothelial cell growth supplements, 100 units/ml penicillin and 100 units/ml streptomycin at 37 °C under 5% CO_2 and 95% air. Passage 2–6 was used for experiments.

For most experiments, after growing to sub-confluence, cells were pretreated with vehicle or various concentrations of COS (50–200 μg/ml) in DMEM-F12 with 10% FBS for 4–24 h. After that, H_2O_2 with a final 400 μM concentration was added to the culture medium without wash for different time intervals until further analysis.

2.3. H_2O_2 scavenging analysis

H_2O_2 scavenging activity of COS was assayed as reported by Ruch et al. with some modification (Singha, Mittala, Kaurb, Batishb, & Kohli, 2009). Briefly, 0.2 ml of different concentrations of COS (50–200 μg/ml) were added to 0.6 ml of H_2O_2 (40 mM) in phosphate-buffered saline (PBS, pH 7.4) and thoroughly mixed. After 30 min incubation without light at room temperature, absorbance of the solution was determined spectrophotometrically at 230 nM against a blank containing COS in PBS without H_2O_2. The percent scavenging of H_2O_2 by COS was calculated according to the following equation, in which A and A_0 were absorbance of samples and control, respectively.

$$\%\ \text{Scavenging of COS} = (A_0 - A)/A_0 \times 100$$

2.4. Determination of cell viability

Cell viability analysis was performed based on the capacity of mitochondrial enzymes to transform MTT to formazan. HUVECs were seeded in 96-well plates at a density of 7.5×10^3 cells/well containing 150 μl of DMEM-F12 with 10% FBS and incubated overnight. After the drug treatment, 100 μl of MTT (5 mg/ml) was added to each well and cells were incubated at 37 °C for 3 h. Next, the culture medium with dye was abandoned and 100 μl of dimethyl sulfoxide was added to dissolve the formazan crystal. The optical density of each well was measured at 490 nm using a Sunrise Remote Microplate Reader (Grodlg, Austria). The viability of HUVECs in each well was presented as percentage of control cells.

2.5. Fluorescent staining of HUVECs with Hoechst 33258

The blue fluorescent dye Hoechst 33258 is sensitive to DNA conformation and chromatin state in cells. Consequently, Hoechst 33258 can be used to detect gradation of nuclear damage. Briefly, HUVECs were cultured in sterile coverslips to 50% confluence. After the drug treatment, cells were washed with PBS and then stained with 1.0 μg/ml Hoechst 33258 in DMEM-F12 with 10% FBS for 20 min at 37 °C. After three washes with PBS, cells were mounted with aqueous mounting media. Photography was performed with a Leica DMRX microscope (Wetzlar, Germany).

2.6. DNA fragmentation assay

For DNA fragmentation assay, cells were washed with PBS and cellular DNA was extracted with Tris–phenol via violent vortex for 10 min. After cell lysate was centrifuged at 12,000*g* for 5 min, the supernatant was collected and precipitated with 100% ethanol at a 1:2 ratio for 10 min. The precipitation as DNA extract was resuspended in sterile water, and DNA samples were applied on 1.5% agarose gel containing 1% GoldView™. The gel was examined and photographed by ultraviolet gel documentation system (Bio-Rad, Hercules, CA, USA).

2.7. Flow cytometric evaluation of cell proliferation, mitochondrial membrane potential and intracellular Ca^{2+} level

The non-fluorescent dye CFSE can be cleaved by intracellular esterase to form fluorescent conjugates with amines and the dye-protein adducts are equally inherited by daughter cells after cell division. Therefore, proliferation activity of cells can be accurately evaluated by the average fluorescent intensity, which is negatively correlated with the divided cell number. For flow cytometric evaluation of cell proliferation, HUVECs were labeled with CFSE (20 μM) in DMEM-F12 (10% FBS) for 5 h at 37 °C. Then, the culture medium was washed away and cells were treated with COS and/or H_2O_2. After the treatment, cells were washed, harvested and resuspended with PBS. The fluorescence in cells was quantitatively analyzed at an emission wavelength of 530 nm and an excitation wavelength of 480 nm using a Vantage SE flow cytometer with

fluorescence activated cell sorting (FACS) system (Becton Dickinson, San Jose, CA, USA).

Mitochondrial membrane potential of HUVECs was assessed by using MitoProbe™ JC-1 Assay Kit. JC-1 exhibits potential-dependent accumulation in mitochondria as indicated by a fluorescence emission shift from green to red. Consequently, mitochondrial depolarization can be assessed by a decrease in the red/green fluorescence intensity ratio. After the drug treatment, cells were washed and incubated with DMEM-F12 (10% FBS) containing 2 μg/ml of JC-1 for 20 min at 37 °C. Finally, cells were washed, harvested, re-suspended with PBS and analyzed on a flow cytometer as before.

The non-fluorescent dye fluo-3 AM was used for intracellular Ca^{2+} detection. Upon diffusion into cells, fluo-3 AM can be cleaved into fluo-3 by endogenous esterases and trapped inside the cells. After binding to Ca^{2+}, fluo-3 elicits fluorescent light, which is proportional to the intracellular Ca^{2+} level. In brief, after the drug treatment, cells were washed and incubated with DMEM-F12 (10% FBS) containing 0.5 μM of fluo-3 AM for 1 h at 37 °C. Next, cells were washed, harvested, re-suspended with PBS and analyzed on a flow cytometer as before.

2.8. Reverse transcription-polymerase chain reaction (RT-PCR)

Total RNA was extracted from HUVECs using TRIZOL (Takara, Dalian, China). The quantity of RNA isolates was determined spectrophotometrically using a DNA/RNA Gene-Quant Calculator (Amersham Biosciences, USA). Reverse transcription was performed in 20 μl of reaction mixture containing 2 μg of total RNA, 5.0 units of AMV reverse transcriptase, 50 pmol of oligo-dT primer, 40 nmol of dNTP mixture, 40 units of RNase inhibitor, 4 μl of 5 × RT buffer (Bioer, Hangzhou, China) at 42 °C for 1 h and 95 °C for 5 min. The following primers for RT-PCR were used: Bcl-2 (200 bp): sense 5′-GAA GGA ATG TTG CAT GAG TCG GAT C-3′; Antisense: 5′-CCT AGA AAT GTA GGC GTC AAG GGA A-3′, Bax (153 bp): sense 5′-GAT CGA GCA GGG CGA ATG GG-3′; Antisense 5′-CAC GGC GGC AAT CAT CCT CT-3′, GAPDH (230 bp): sense 5′-CTC TCT GCT CCT CCT GTT CGA CAG-3′; Antisense 5′-GTG GAA TCA TAT TGG AAC ATG T-3′. RT-PCR analysis was performed in 20 μl of reaction mixture containing 1 μl of cDNA reaction mixture, 10 nmol of dNTP mixture, 10 pmol of sense and antisense primers, and two units of BioReady rTaq polymerase (Bioer, Hangzhou, China). The thermal cycling program was as follows: 4 min at 94 °C for initial denaturation; 30 cycles × 30 s at 94 °C, 30 s at 54 °C, and 30 s at 72 °C for Bcl-2 and GAPDH; 30 cycles × 30 s at 94 °C, 30 s at 59 °C, and 30 s at 72 °C for Bax. For PCR product analysis, 6 μl of each reaction mixture was electrophoresed on 1.5% agarose gel containing 1% GoldView™. Band intensity was analyzed with ImageJ system (NIH, USA) and presented as a percentage of GAPDH expression.

2.9. Western blot analysis

For isolation of total protein extract, HUVECs were washed with ice-cold PBS and lysed in RIPA lysis buffer (50 mM Tris with pH 7.4, 150 mM NaCl, 1% Triton X-100, 1% sodium deoxycholate, 0.1% sodium dodecyl sulphate and 0.05 mM EDTA) for 15 min on ice, and cell lysate was centrifuged at 12,000*g* for 10 min at 4 °C. The supernatant was collected and protein content of extracted samples was measured using bicinchoninic acid protein assay kit (BioMed, Beijing, China). All samples were stocked at −80 °C for further experiments.

Levels of target proteins including caspase-3, p-p38, p38, p-Akt, Akt and GAPDH were determined by Western blot analysis using the respective antibodies stated above. Briefly, total cell lysate was boiled in 5 × loading buffer (125 mM Tris–HCl, pH 6.8, 10% SDS, 8% dithiothreitol, 50% glycerol and 0.5% bromchlorphenol blue) for 10 min. Equal amount of proteins (50 μg) was subjected to 8–12% SDS–polyacrylamide gel electrophoresis and transferred to polyvinylidene fluoride membranes. The membranes were blocked with 5% skim milk in PBS with 0.1% Tween 20 (PBST) for 1 h, and incubated with primary antibodies overnight at 4 °C. Antibodies were detected by means of HRP-conjugated secondary antibody for 1 h at room temperature. Immunoreactive bands were visualized using enhanced chemiluminescence reagents (ECL) and densitometric analysis was performed with the use of PDI Imageware System (Bio-Rad, Hercules, CA, USA).

2.10. Statistics

Values are expressed as mean ± SD. Statistical comparisons were performed using SPSS 10.0 package (SPSS Inc., Chicago, IL, USA). One-way ANOVA and Student's *t*-test followed by a Bonferroni correction were carried out to determine statistical significance. Differences were considered significant at $P < 0.05$.

3. Results

3.1. COS exhibit no scavenging activity against H_2O_2

We first assessed the direct scavenging activity of COS against H_2O_2 in a cell-free assay. It was observed that COS (50, 100 and

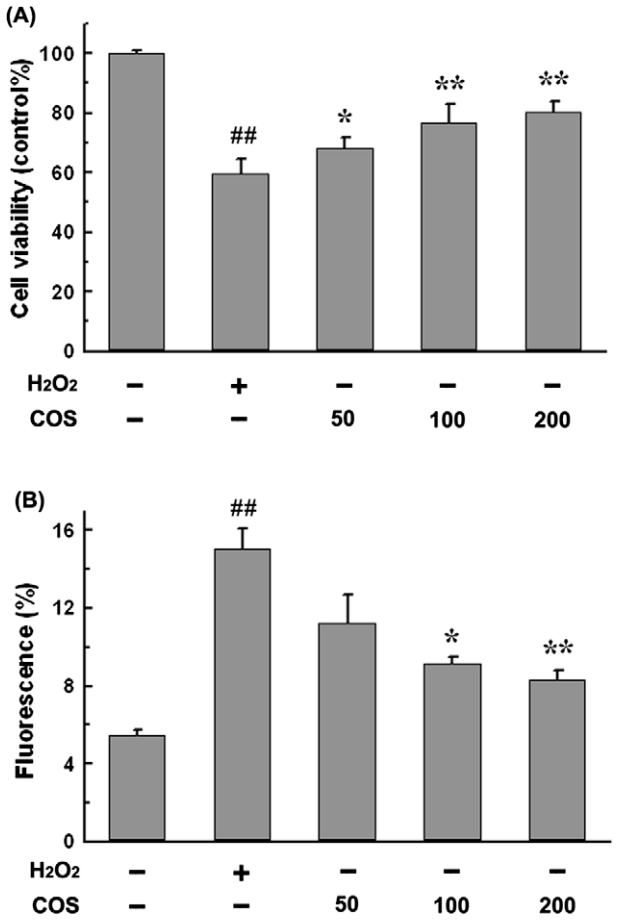

Fig. 1. Effect of COS on H_2O_2-induced decrease in cell viability (A) and proliferation (B) of HUVECs. Cells were pretreated with COS (50–200 μg/ml) for 4 h and then exposed to H_2O_2 (400 μM) for 20 h. After the treatment, cell viability was determined by MTT analysis ($n = 5$) and cell proliferation ($n = 3$) was performed by flow cytometry as described in Section 2. Data are expressed as means ± SD. $^{\#\#}P < 0.01$ compared to the vehicle-treated group; $^{*}P < 0.05$ and $^{**}P < 0.01$ compared to the H_2O_2-treated group.

200 μg/ml) showed no scavenging activity against H_2O_2 (40 mM) after 30 min incubation (data not shown). The results indicate that no reaction will occur when COS are incubated with H_2O_2.

3.2. COS ameliorate H_2O_2-induced decrease in cell viability and proliferation of HUVECs

Effect of COS on cell viability of H_2O_2-induced HUVECs was evaluated by MTT conversion test. Cells were pretreated with COS (50–200 μg/ml) for 4 h and then exposed to H_2O_2 (400 μM) for 20 h. As shown in Fig. 1A, the cell viability was decreased to 59.9 ± 4.6% ($P < 0.01$) of the vehicle-treated group after cells were exposed to H_2O_2. After COS (50, 100 and 200 μg/ml) pretreatment, the reduced viabilities of HUVECs were dose-dependently increased to 68.2 ± 3.7% ($P < 0.05$), 76.9 ± 6.0% ($P < 0.01$) and 80.3 ± 3.8% ($P < 0.01$) of the vehicle-treated group, respectively. Additionally, no difference was detected in cell viability between cells treated with COS (25–200 μg/ml) alone and vehicle (data not shown).

Effect of COS on cell proliferation of H_2O_2-induced HUVECs was investigated using the intracellular dye CFSE. With successive cell division, the average fluorescence in daughter cells will be gradually lessened and indirectly reflect the proliferation activity. Results in Fig. 1B show that the fluorescent intensity in HUVECs was minimal in the vehicle-treated group (5.5 ± 0.2%) and a pronounced increase was observed after H_2O_2 exposure (400 μM) for 20 h (15.1 ± 1.1%, $P < 0.01$, vs. the vehicle-treated group). In contrast, pretreatment with COS (50, 100 and 200 μg/ml) for 4 h reduced the fluorescent intensities in a dose-dependent manner (50 μg/ml, 11.3 ± 1.5%, $P = 0.08$; 100 μg/ml, 9.2 ± 0.4%, $P < 0.05$; 200 μg/ml, 8.4 ± 0.4%, $P < 0.01$, vs. the H_2O_2-treated group).

3.3. COS inhibit H_2O_2-induced nuclear damage in HUVECs

To investigate the inhibitory effect of COS on H_2O_2-induced nuclear damage in HUVECs, the morphological analysis of HUVECs was conducted by Hoechst 33258 staining and agarose gel electrophoresis of DNA fragmentation. HUVECs was pretreated with COS (50, 100 and 200 μg/ml) for 4 h and then exposed to H_2O_2 (400 μM) for 20 h. Results in Fig. 2A show that the condensed chromatin of H_2O_2-induced HUVECs was stained more brightly by Hoechst 33258 than that of vehicle-treated cells, whereas pretreatment with 200 μg/ml of COS evidently reverted the strong staining of nuclear chromatin in H_2O_2-induced HUVECs. In addition, a genomic DNA ladder formation was clearly observed when cells were treated with 400 μM of H_2O_2 for 20 h, and was inhibited by COS pretreatment from 50 to 200 μg/ml (Fig. 2B).

3.4. COS suppress H_2O_2-induced loss of mitochondrial membrane potential in HUVECs

Mitochondrial membrane potential, expressed as JC-1 fluorescent intensity, is an important parameter reflecting the membrane integrity of mitochondria. As indicated in Fig. 3, after H_2O_2 (400 μM) exposure for 20 h, the fluorescent intensity of HUVECs was increased from 2.6 ± 0.3% to 21.4 ± 1.1% ($P < 0.01$, vs. the vehicle-treated group), while COS (50, 100 and 200 μg/ml) pretreatment for 4 h inhibited H_2O_2-induced increase in fluorescent intensity (50 μg/ml, 11.8 ± 1.2%, $P < 0.01$; 100 μg/ml, 8.5 ± 0.3%, $P < 0.01$; 200 μg/ml, 8.7 ± 0.7%, $P < 0.01$, vs. the H_2O_2-treated group).

3.5. COS block H_2O_2-induced Ca^{2+} influx in HUVECs

Because cytosolic Ca^{2+} plays an important role in regulation of cell growth and death, we determined the blocking effect of COS on H_2O_2-induced Ca^{2+} influx in HUVECs. Cells were pretreated with COS (50, 100 and 200 μg/ml) for 18 h and then exposed to H_2O_2 (400 μM) for 6 h. As shown in Fig. 4, H_2O_2 exposure significantly increased the Ca^{2+} influx in HUVECs (22.8 ± 2.1%, $P < 0.01$, vs. the vehicle-treated group). On the contrary, pretreatment with COS (50–200 μg/ml) blocked the strengthened Ca^{2+} influx in cells induced by H_2O_2 (50 μg/ml, 12.6 ± 0.8%, $P < 0.05$; 100 μg/ml, 8.5 ± 1.0%, $P < 0.01$; 200 μg/ml, 9.1 ± 0.9%, $P < 0.01$, vs. the H_2O_2-treated group).

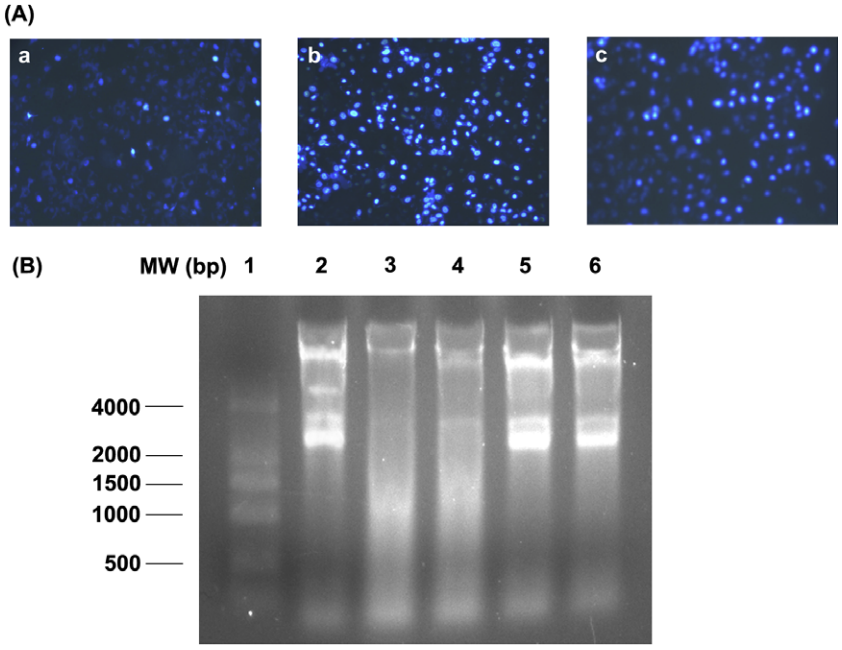

Fig. 2. Morphological analysis of HUVECs treated with vehicle, COS and/or H_2O_2. Cells were pretreated with COS (50–200 μg/ml) for 4 h and then exposed to H_2O_2 (400 μM) for 20 h. (A) Fluorescent staining of nucleus by Hoechst 33258: (a) vehicle-treated cells; (b) cells exposed to 400 μM of H_2O_2 for 20 h; and (c) cells pretreated with 200 μg/ml of COS for 4 h before exposed to 400 μM of H_2O_2 for 20 h. (B) Agarose gel electrophoresis of DNA fragmentation: Lane 1, DNA ladder marker; Lane 2, vehicle-treated cells; Lane 3, cells exposed to 400 μM of H_2O_2 for 20 h; and Lane 4–6, cells separately pretreated with 50, 100 and 200 μg/ml of COS for 4 h before exposed to 400 μM of H_2O_2 for 20 h.

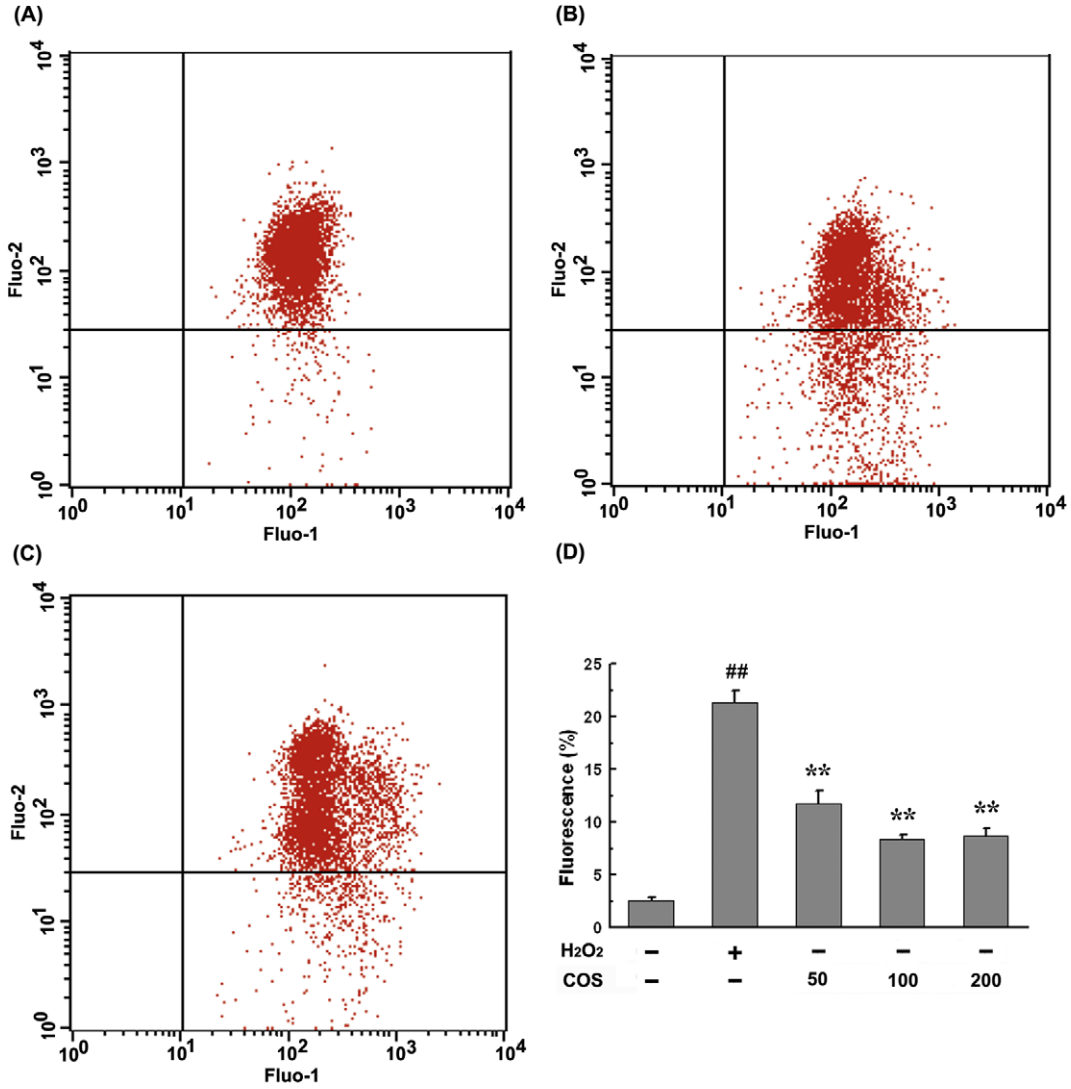

Fig. 3. Effect of COS on loss of mitochondrial membrane potential in H_2O_2-induced HUVECs. Cells were pretreated with COS (50–200 μg/ml) for 4 h and then exposed to H_2O_2 (400 μM) for 20 h. After the treatment, mitochondrial membrane potential in HUVECs was performed by flow cytometry as described in Materials and methods. (A–C) Representative flow cytometric histograms of vehicle-treated cells, cells exposed to 400 μM of H_2O_2 for 20 h and cells pretreated with 200 μg/ml of COS for 4 h before exposed to 400 μM of H_2O_2 for 20 h, respectively. (D) Fluorescent intensities of HUVECs treated with vehicle, COS and/or H_2O_2. Data are expressed as means ± SD ($n = 3$). $^{\#\#}P < 0.01$ compared to the vehicle-treated group and $^{**}P < 0.01$ compared to the H_2O_2-treated group.

3.6. COS up-regulate Bcl-2 mRNA level and down-regulate Bax mRNA level in H_2O_2-induced HUVECs

Since COS at 200 μg/ml demonstrated the most significant protective effect on H_2O_2-induced oxidative damage in previous experiments, we conducted all further studies using this dose only. To explore the molecular mechanisms underlining inhibitory effect of COS on H_2O_2-induced apoptosis, we examined mRNA expression of Bcl-2 in HUVECs by RT-PCR analysis. HUVECs were pretreated with COS (200 μg/ml) for 18 h and then exposed to H_2O_2 (400 μM) for 6 h. As expected, Bcl-2 mRNA level was decreased to 55.4 ± 3.9% ($P < 0.05$) of the vehicle-treated group after H_2O_2 exposure. Contrary to this, COS (200 μg/ml) pretreatment statistically increased the Bcl-2 mRNA level (137.4 ± 5.2% of the H_2O_2-treated group, $P < 0.05$) (Fig. 5A).

We also measured the mRNA expression of Bax, a pro-apoptotic protein in Bcl-2 family. As indicated in Fig. 5A, Bax mRNA level in HUVECs was increased to 211.2 ± 21.1% ($P < 0.01$) of the vehicle-treated group after exposed to 400 μM of H_2O_2 for 6 h, and COS (200 μg/ml) pretreatment for 6 h reversed the over-expression of Bax mRNA by H_2O_2 challenge (35.3 ± 2.5% of the H_2O_2-treated group, $P < 0.01$).

3.7. COS inhibit H_2O_2-induced caspase-3 activation in HUVECs

Caspase-3 is a key "executer" protease of endothelial cell apoptosis (Irani, 2000), and we thus investigated the effect of COS on H_2O_2-induced activation of caspase-3 in HUVECs. Cells were pretreated with COS (200 μg/ml) for 4 h and then exposed to H_2O_2 (400 μM) for 20 h. Western blot analysis revealed that the amount of cleaved caspase-3 in H_2O_2-induced HUVECs was markedly increased (514.7 ± 66.9% of the vehicle-treated group, $P < 0.01$) (Fig. 5B). However, COS (200 μg/ml) pretreatment attenuated the H_2O_2-induced caspase-3 activation (62.7 ± 4.4% of the H_2O_2-treated group, $P < 0.05$).

3.8. COS down-regulate p-p38 MAPK level and up-regulate p-Akt level in H_2O_2-induced HUVECs

To determine the up-stream signaling pathways by which COS exert their anti-apoptotic effects, the activation of p38 MAPK and Akt was assessed. HUVECs were pretreated with COS (200 μg/ml) for 24 h and then exposed to H_2O_2 (400 μM) for 30 min. As shown in Fig. 6A, H_2O_2 exposure led to an increase in the level of p-p38

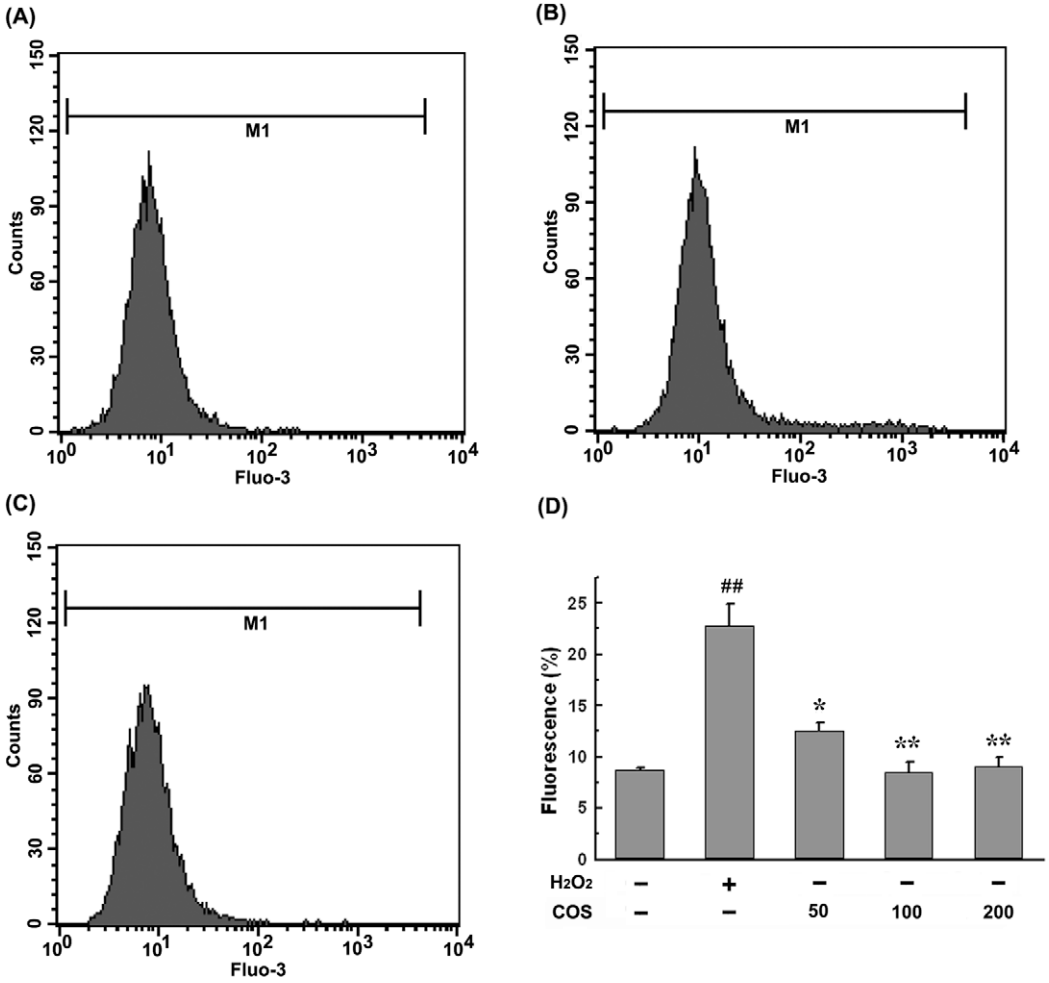

Fig. 4. Effect of COS on Ca^{2+} influx in H_2O_2-induced HUVECs. Cells were pretreated with COS (50–200 μg/ml) for 18 h and then exposed to H_2O_2 (400 μM) for 6 h. After the treatment, cytosolic Ca^{2+} level in HUVECs was determined by flow cytometry as described in Section 2. (A–C) Representative flow cytometric histograms of vehicle-treated cells, cells exposed to 400 μM of H_2O_2 for 6 h and cells pretreated with 200 μg/ml of COS for 18 h before exposed to 400 μM of H_2O_2 for 6 h, respectively. (D) Fluorescent intensities of HUVECs treated with vehicle, COS and/or H_2O_2. Data are expressed as means ± SD ($n = 3$). $^{\#\#}P < 0.01$ compared to the vehicle-treated group; $^{*}P < 0.05$ and $^{**}P < 0.01$ compared to the H_2O_2-treated group.

(303.9 ± 42.4% of the vehicle-treated group, $P < 0.01$), which was inhibited by pretreatment with COS (39.9 ± 2.4% of the H_2O_2-treated group, $P < 0.01$). On the contrary, the level of p-Akt in HUVECs was decreased to 15.6 ± 1.2% ($P < 0.01$) of the vehicle-treated group after H_2O_2 exposure, while COS pretreatment alleviated this down-regulation of p-Akt by H_2O_2 (468.7 ± 37.5% of the H_2O_2-treated group, $P < 0.01$) (Fig. 6B).

3.9. Activation of caspase-3 is suppressed by p38 MAPK inhibitor (SB203580) and elevated by PI3K inhibitor (LY294002) in H_2O_2-induced HUVECs

To document whether COS inhibit H_2O_2-induced activation of caspase-3 in HUVECs through the regulation of p38 MAPK and PI3K/Akt signaling pathways, specific p38 MAPK inhibitor, SB203580 and PI3K inhibitor, LY294002, were used in this study. HUVECs were pretreated with SB203580 (30 μM) or LY294002 (50 μM) for 1 h, and then exposed to H_2O_2 (400 μM) for 20 h. Results in Fig. 7A indicate that H_2O_2-induced high expression of cleaved caspase-3 in HUVECs was reduced to 72.9 ± 3.6% of the H_2O_2-treated group ($P < 0.05$) by pretreatment with SB203580, yet pretreatment with LY294002 not only induced a higher level of cleaved caspase-3 (158.8 ± 17.5% of the vehicle-treated group, $P < 0.05$) in vehicle-treated cells, but further elevated the increased level of cleaved caspase-3 (147.3 ± 13.3% of the H_2O_2-treated group, $P < 0.05$) in H_2O_2-induced HUVECs (Fig. 7B).

4. Discussion

Enhanced oxidative damage to ECs by ROS has been marked as a prominent feature of cardiovascular diseases (Fasanaro et al., 2006). Many pathogenic factors such as cytokines, endotoxin and shear stress were reported to induce high levels of ROS and subsequent apoptosis in ECs (Kim, Shin, Choi, & Hong, 2002; Xia et al., 2006). Thus, pharmacological interventions targeting the inhibition of oxidative stress-induced EC apoptosis may be a key step in prevention of cardiovascular diseases. So far, some anti-oxidative agents against scavenging ROS, including Vitamin E, flavanoids and phenolic acids, have displayed suppressive effects on H_2O_2-induced EC apoptosis (Lin, Liu, Gan, & Ding, 2007; Liu et al., 2007; Marsh, Laursen, Pat, Gobe, & Coombes, 2005). In this study, we for the first time demonstrate that COS can protect HUVECs from H_2O_2-induced apoptosis.

Cultured HUVECs are particularly prone to oxidative damage and H_2O_2 has been extensively used as an apoptotic inducer in *in vitro* models. After exposed to high amount of H_2O_2, HUVECs will suffer remarkable cytotoxicity, which is characterized by losses of cell viability and proliferative activity, the initial events in process

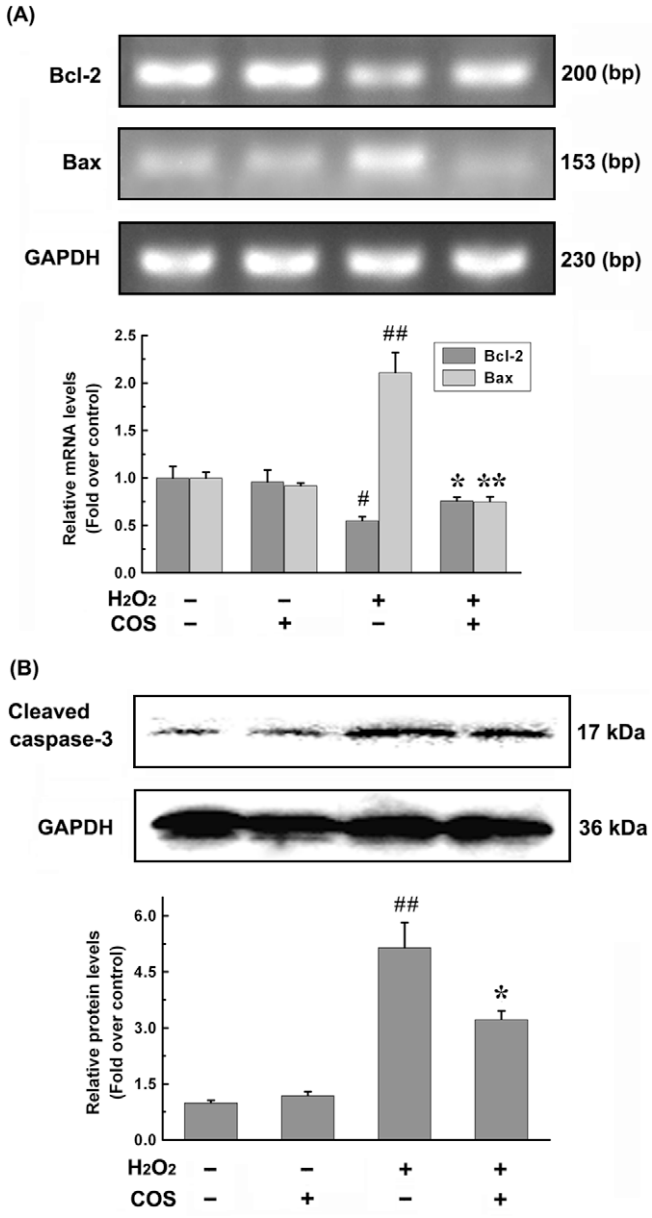

Fig. 5. Effect of COS on mRNA levels of Bcl-2 and Bax (A), and protein level of cleaved caspase-3 (B) in H_2O_2-induced HUVECs. (A) Cells were pretreated with COS (200 μg/ml) for 18 h and then exposed to H_2O_2 (400 μM) for 6 h. After the treatment, Bcl-2 and Bax mRNA levels were determined by RT-PCR analysis as described in Materials and methods. (B) Cells were pretreated with COS (200 μg/ml) for 4 h and then exposed to H_2O_2 (400 μM) for 20 h. After the treatment, protein level of cleaved caspase-3 was measured by Western blot analysis as described in Materials and methods. Data are expressed as means ± SD ($n = 3$). $^{\#}P < 0.05$, $^{\#\#}P < 0.01$ compared to the vehicle-treated group and $^{*}P < 0.05$, $^{**}P < 0.01$ compared to the H_2O_2-treated group.

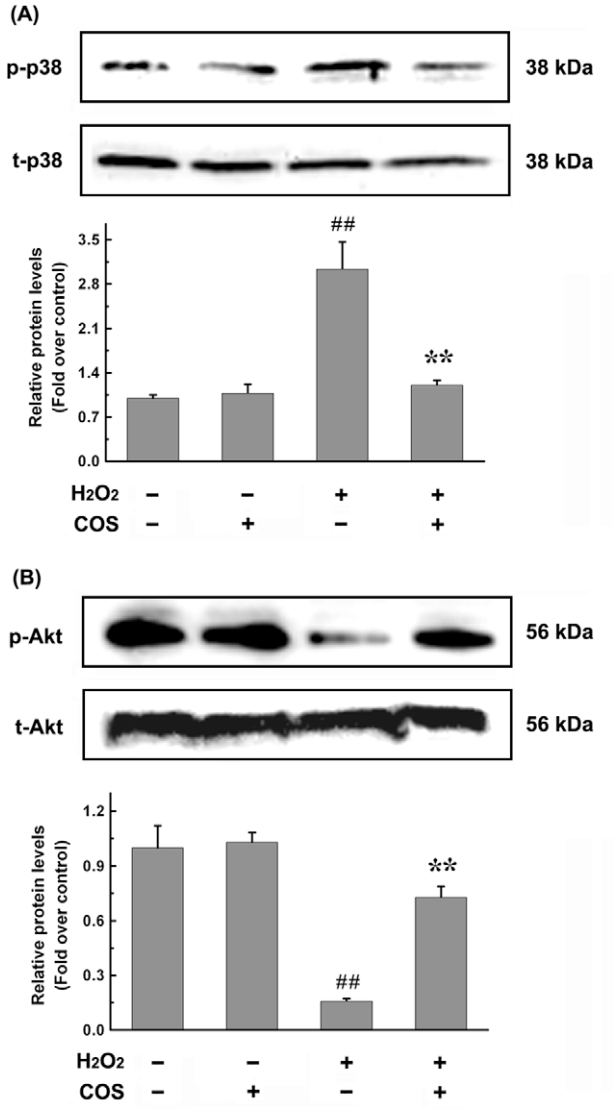

Fig. 6. Effect of COS on phosphorylated levels of p38 MAPK (A) and Akt (B) in H_2O_2-induced HUVECs. P-p38: phosphorylated p38 MAPK; p-Akt: phosphorylated Akt. Cells were pretreated with COS (200 μg/ml) for 24 h and then exposed to H_2O_2 (400 μM) for 30 min. After the treatment, protein levels of p-p38 and p-Akt were determined by Western blot analysis as described in Section 2. Data are expressed as means ± SD ($n = 3$). $^{\#\#}P < 0.01$ compared to the vehicle-treated group and $^{**}P < 0.01$ compared to the H_2O_2-treated group.

of apoptosis (Hale et al., 1996). As many papers have reported, we here found that the viability and proliferation of HUVECs were significantly decreased after H_2O_2 challenge, and this decrease were partly abrogated by COS pretreatment. Morphological analysis showed similar results, in which COS pretreatment lessened the strong staining of nuclear chromatin by H_2O_2 challenge, accompanied by an ameliorated nuclear damage after COS pretreatment. Noticeably, it seemed that COS failed to work through directly degrading H_2O_2, because no reaction between COS and H_2O_2 was observed in cell-free assay. From these results, it can be speculated that COS effectively ameliorated H_2O_2-induced cytotoxicity of HUVECs by certain intracellular mechanisms.

Mitochondria are complex cell organelles and play essential roles in maintenance of cell survival. Mitochondrial membrane potential has been regarded as a central bioenergy parameter, which controls ATP synthesis, respiratory rate and production of ROS (Chai, Wang, Huang, Xie, & Fu, 2008). The signs of cell death were preceded by mitochondrial impairment such as a loss of mitochondrial membrane potential (Chen et al., 2006). It has been shown that the so-called intrinsic program of apoptosis was mainly triggered by the mitochondrial pathway (Wang, 2001). Therefore, to elucidate the mechanisms of action for COS against HUVEC apoptosis after H_2O_2 exposure, we first determined the inhibitory effect of COS on loss of mitochondrial membrane potential. Indeed, COS pretreatment greatly prevented HUVECs from H_2O_2-induced reduction of mitochondrial membrane potential, indicating that inhibitory effect of COS on HUVEC apoptosis was relative to their protection of mitochondria. Similar findings were obtained by Chen et al. (2006) who have proved that carboxymethyl-chitosan

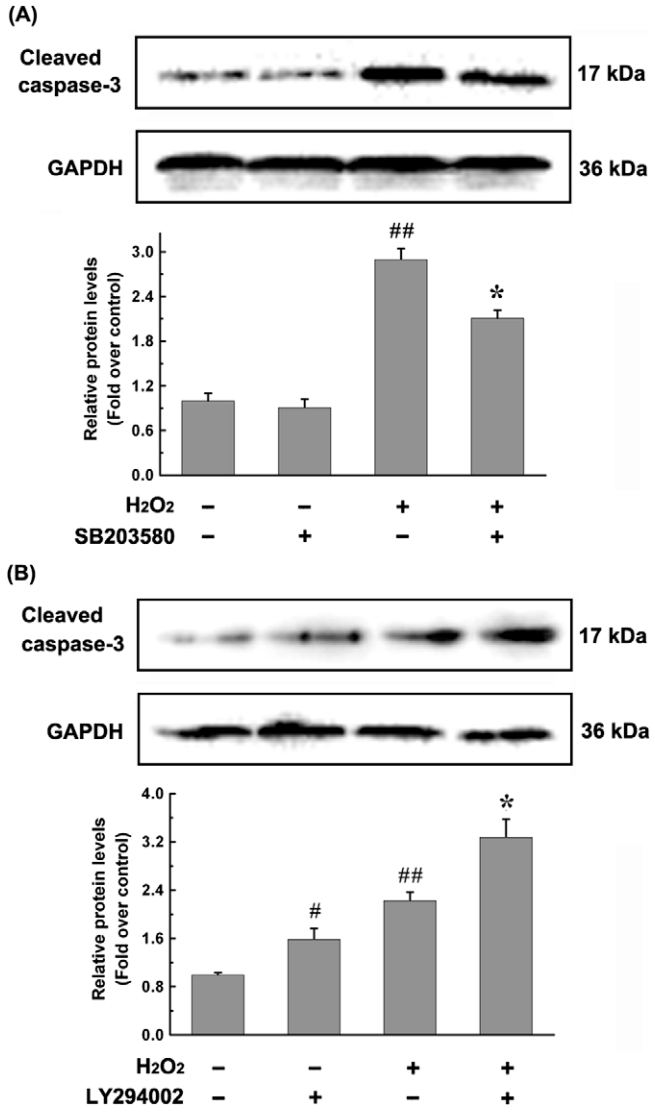

Fig. 7. Effects of p38 MAPK inhibitor, SB203580 (A) and PI3K inhibitor, LY294002 (B) on H_2O_2-induced activation of caspase-3 in HUVECs. Cells were pretreated with SB203580 (30 μM) or LY294002 (50 μM) for 1 h, and then exposed to H_2O_2 (400 μM) for 20 h. After the treatment, protein level of cleaved caspase-3 was measured by Western blot analysis as described in Materials and methods. Data are expressed as means ± SD ($n = 3$). $^{\#}P < 0.05$, $^{\#\#}P < 0.01$ compared to the vehicle-treated group and $^{*}P < 0.05$ compared to the H_2O_2-treated group.

suppressed the decrease in mitochondrial membrane potential of IL-β-induced chondrocytes.

Ca^{2+} is a primary indicator of cell activation and function, and accumulation of cytosolic Ca^{2+} is intricately linked with ROS production, mitochondrial function and cell death (Parekh & Putney, 2005; Tan, Sagara, Liu, Maher, & Schubert, 1998). It was reported that loss of mitochondrial function led to an increase in cytosolic Ca^{2+}, which subsequently initiated the occurrence of cell apoptosis (Luo, Bond, & Ingram, 1997). Moreover, increased Ca^{2+} influx might regulate the apoptotic process by modulating activities of PI3K/Akt and MAPK cascades that are vital to cell survival or death (Chen, Nguyen, Pike, & Russo-Neustadt, 2007). In previous studies, COS (250 kDa, deacetylation degree of 92.3%) were found to depress glutamate-induced elevation of intracellular Ca^{2+} level in cultured hippocampal neurons (Zhou, Yang, Gu, & Ding, 2008). To date, the elevation of Ca^{2+} during oxidative damage has been well documented in HUVECs after H_2O_2 exposure (Xu et al., 2008a; Xu et al., 2008b). Consistently, our present study showed that the up-regulation of cytosolic Ca^{2+} level in H_2O_2-induced HUVECs was inhibited by COS pretreatment. In addition, the Ca^{2+} level in vehicle-treated cells was not influenced by COS (data no shown). It is apparent that there is direct involvement of Ca^{2+} channel in protective mechanisms of COS against H_2O_2-inducd apoptosis in HUVECs.

The members of Bcl-2 family act as anti- or pro-apoptotic regulators that are involved in a wide variety of cellular activities. Bcl-2 is the first gene shown to be a negative regulator of cell death and protects cells from undergoing apoptosis induced by exogenous stimuli, whereas Bax is a pro-apoptotic regulator that promotes or accelerates cell death (Guan, Jiang, Bao, & An, 2006; Vaux, Cory, & Adams, 1988). The abilities of Bcl-2 and Bax to control cell proliferation or death are intimately associated with mitochondrial function (Xu et al., 2008a, 2008b). It is now clear that, under pathological conditions, Bcl-2 reduces apoptosis through preventing the decrease of mitochondrial membrane potential and Bax promotes apoptosis by inducing mitochondrial depolarization (Guan et al., 2006; Jürgensmeier et al., 1998). On the other hand, damaged mitochondria will ultimately result in the activation of caspase cascade, which is the main executor to induce cell apoptosis by cleaving a critical set of cellular proteins (Moriue et al., 2008). In the current study, COS showed inhibitory effects on down-regulation of Bcl-2 and up-regulation of Bax at mRNA levels in H_2O_2-induced HUVECs. Furthermore, the level of cleaved caspase-3 protein was also decreased by COS pretreatment. The results implied involvement of these down-stream apoptotic regulators in suppressive effect of COS on HUVEC apoptosis. Interestingly, in our anti-tumor studies, COS displayed a pro-apoptotic effect in human hepatocellular carcinoma cells, in which Bcl-2 expression was suppressed and Bax expression was induced (Xu et al., 2008a, 2008b). These contradictory effects of COS may be due to different cell types and the changed cellular redox status.

Among cell signaling pathways in ECs, MAPKs and PI3K/Akt is known to be essential for the survival or death of ECs (Liu et al., 2007). It has been confirmed that p38 MAPK served as a pro-apoptosis signal and PI3K/Akt as pro-survival signals in oxidative stress-stimulated ECs (Hwang & Yen, 2009; Irani, 2000), and these effects are mediated by apoptosis-related transcription factors of Bcl-2 family (Maheshwari, Misro, Aggarwal, Sharma, & Nandan, 2009; Morello, Perino, & Hirsch, 2009). Thus, in this study, we chose the two well-established components in apoptotic signaling pathways, p38 MAPK and PI3K/Akt, as indicators to verify the protective effect of COS on H_2O_2-induced HUVEC apoptosis. Our findings suggest that COS pretreatment was capable of inhibiting p38 MAPK phosphorylation and enhancing Akt phosphorylation in H_2O_2-induced HUVECs. More importantly, pretreatment with p38 MAPK inhibitor, SB203580, partly blocked H_2O_2-induced activation of caspase-3 and pretreatment with PI3K inhibitor, LY294002, showed an aggravated activation of caspase-3. These results show that the anti-apoptotic activity of COS against H_2O_2-induced HUVECs may be positively correlated with suppressed caspase-3 activation which was regulated by the phosphorylation of p38 MAPK and PI3K/Akt.

Apoptosis occur mainly through two apoptotic pathways, i.e., the intrinsic mitochondria-mediated pathway such as Bcl-2 family-related signals and the extrinsic death receptor-induced pathway generally associated with Ca^{2+}, MAPKs, PI3K/Akt and oxidative stress (Zou, Yue, Khuri, & Sun, 2008). The two pathways independently or synergistically regulate cell survival or death. Thus, the protective effect of COS on H_2O_2-induced HUVEC apoptosis may result from a synergistical action via the molecules involved in this study. Regretfully, the action mechanisms of COS, as summarized in Fig. 8, only reflected signaling pathways in cytoplasma of HUVECs, and what happen on cell membrane should be further investigated in future studies.

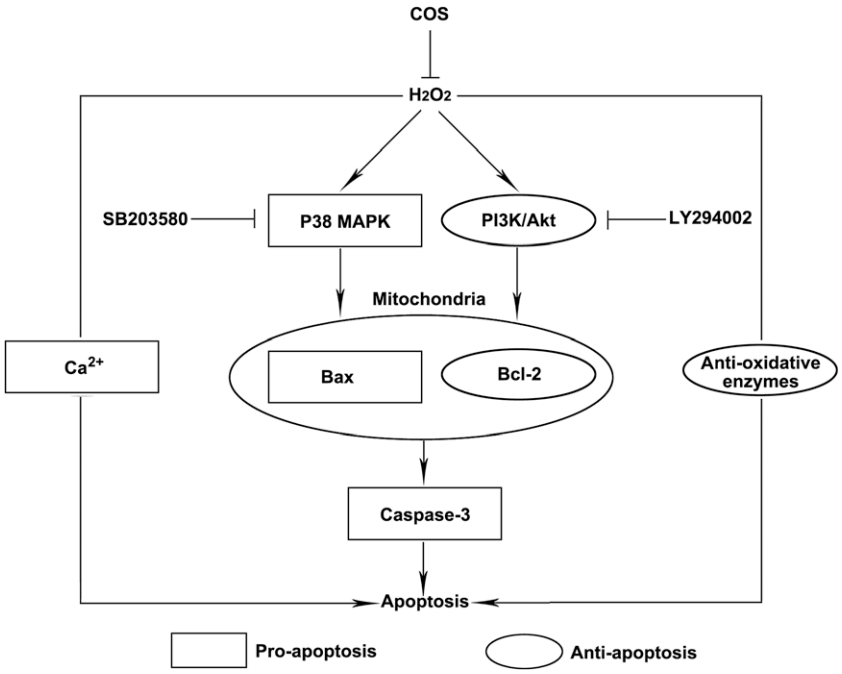

Fig. 8. Proposed mechanisms mediating H_2O_2-induced HUVEC apoptosis and effect of COS in this process.

Based on these results, it can be concluded that COS exerted remarkable protective effect on H_2O_2-induced HUVEC apoptosis. In our previous studies, COS at 100–200 μg/ml showed marked protective effects on H_2O_2-induced oxidative damage in endothelial cells, comparable to that by Vitamin C (250 μg/ml) (Liu et al., 2009). Collectively, there have at least three parallel regulation mechanisms that contribute to the anti-apoptotic effect of COS (Fig. 8): (1) down-regulation of cytosolic Ca^{2+} level; (2) blockade of mitochondria-dependent apoptosis program including the change of mitochondrial membrane potential, activation of Bcl-2 and Bax, cleaving of caspase-3 protein, and participation of p38 MAPK and PI3K/Akt signaling pathways; and (3) restoration of cellular anti-oxidative enzyme activities. In consideration of the good anti-apoptotic activity of COS in HUVECs, our findings shed light on the potential application for COS in treatment of oxidative stress-induced cardiovascular diseases.

Acknowledgments

This work was supported by National Programs for High Technology Research and Development (863 Programs, 2006AA10 0313 and 2007AA10Z343), and by Science Fund of Chongqing Medical University, China (XBZD200806).

References

Arvanitoyannis, I. S., Nakayama, A., & Aiba, A. I. (1998). Chitosan and gelatin based edible films: State diagrams, mechanical and permeation properties. *Carbohydrate Polymers, 37*, 371–382.

Cai, H. (2005). Hydrogen peroxide regulation of endothelial function: Origins, mechanisms, and consequences. *Cardiovascular Research, 68*, 26–36.

Chai, H., Wang, Q., Huang, L., Xie, T., & Fu, Y. (2008). Ginsenoside Rb1 inhibits tumor necrosis factor-alpha-induced vascular cell adhesion molecule-1 expression in human endothelial cells. *Biological & Pharmaceutical Bulletin, 31*, 2050–2056.

Chen, M. J., Nguyen, T. V., Pike, C. J., & Russo-Neustadt, A. A. (2007). Norepinephrine induces BDNF and activates the PI-3K and MAPK cascades in embryonic hippocampal neurons. *Cellular Signaling, 19*, 114–128.

Chen, Q., Liu, S. Q., Du, Y. M., Peng, H., & Sun, L. P. (2006). Carboxymethyl-chitosan protects rabbit chondrocytes from interleukin-1beta-induced apoptosis. *European Journal of Pharmacology, 541*, 1–8.

Du, Y. Z., Wang, L., Yuan, H., Wei, X. H., & Hu, F. Q. (2009). Preparation and characteristics of linoleic acid-grafted chitosan oligosaccharide micelles as a carrier for doxorubicin. *Colloids and Surfaces B: Biointerfaces, 69*, 257–263.

Fasanaro, P., Magenta, A., Zaccagnini, G., Cicchillitti, L., Fucile, S., Eusebi, F., et al. (2006). Cyclin D1 degradation enhances endothelial cell survival upon oxidative stress. *Journal of the Federation of American Societies for Experimental Biology, 20*, 1242–1244.

Griendling, K. K., & FitzGerald, G. A. (2003). Oxidative stress and cardiovascular injury: Part I: Basic mechanisms and in vivo monitoring of ROS. *Circulation, 108*, 1912–1916.

Guan, S., Jiang, B., Bao, Y. M., & An, L. J. (2006). Protocatechuic acid suppresses MPP^+-induced mitochondrial dysfunction and apoptotic cell death in PC12 cells. *Food and Chemical Toxicology, 44*, 1659–1666.

Hale, A. J., Smith, C. A., Sutherland, L. C., Stoneman, V. E., Longthorne, V. L., Culhane, A. C., et al. (1996). Apoptosis: Molecular regulation of cell death. *European Journal of Biochemistry, 236*, 1–26.

Halliwell, B. (1997). Antioxidants and human disease: A general introduction. *Nutrition Reviews, 55*, S44–S49 [discussion S49–S52].

Hwang, S. L., & Yen, G. C. (2009). Modulation of Akt, JNK, and p38 activation is involved in citrus flavonoid-mediated cytoprotection of PC12 cells challenged by hydrogen peroxide. *Journal of Agriculture and Food Chemistry, 57*, 2576–2582.

Irani, K. (2000). Oxidant signaling in vascular cell growth, death, and survival: A review of the roles of reactive oxygen species in smooth muscle and endothelial cell mitogenic and apoptotic signaling. *Circulation Research, 87*, 179–183.

Je, J. Y., Park, P. J., & Kim, S. K. (2004). Free radical scavenging properties of hetero-chitooligosaccharides using an ESR spectroscopy. *Food and Chemical Toxicology, 42*, 381–387.

Jürgensmeier, J. M., Xie, Z., Deveraux, Q., Ellerby, L., Bredesen, D., & Reed, J. C. (1998). Bax directly induces release of cytochrome c from isolated mitochondria. *Proceedings of the National Academy of Sciences, 95*, 4997–5002.

Kim, K. Y., Shin, H. K., Choi, J. M., & Hong, K. W. (2002). Inhibition of lipopolysaccharide-induced apoptosis by cilostazol in human umbilical vein endothelial cells. *Journal of Pharmacology and Experimental Therapeutics, 300*, 709–715.

Koo, H. N., Jeong, H. J., Hong, S. H., Choi, J. H., An, N. H., & Kim, H. M. (2002). High molecular weight water-soluble chitosan protects against apoptosis induced by serum starvation in human astrocytes. *Journal of Nutritional Biochemistry, 13*, 245–249.

Lin, R., Liu, J., Gan, W., & Ding, C. (2007). Protective effect of quercetin on the homocysteine-injured human umbilical vein vascular endothelial cell line (ECV304). *Basic & Clinical Pharmacology & Toxicology, 101*, 197–202.

Liu, C. L., Xie, L. X., Li, M., Durairajan, S. S., Goto, S., & Huang, J. D. (2007). Salvianolic acid B inhibits hydrogen peroxide-induced endothelial cell apoptosis through regulating PI3K/Akt signaling. *PLoS One, 2*, e1321.

Liu, H. T., Li, W. M., Xu, G., Li, X. Y., Bai, X. F., Wei, P., et al. (2009). Chitosan oligosaccharides attenuate hydrogen peroxide-induced stress injury in human umbilical vein endothelial cells. *Pharmacological Research, 59*, 167–175.

Luo, T., & Xia, Z. (2006). A small dose of hydrogen peroxide enhances tumor necrosis factor-alpha toxicity in inducing human vascular endothelial cell apoptosis: Reversal with propofol. *Anesthesia & Analgesia, 103*, 110–116.

Luo, Y., Bond, J. D., & Ingram, V. M. (1997). Compromised mitochondrial function leads to increased cytosolic calcium and to activation of MAP kinases. *Proceedings of the National Academy of Sciences, 94*, 9705–9710.

Maheshwari, A., Misro, M. M., Aggarwal, A., Sharma, R. K., & Nandan, D. (2009). Pathways involved in testicular germ cell apoptosis induced by H_2O_2 in vitro. *Federation of European Biochemical Societies Journal, 276*, 870–881.

Marsh, S. A., Laursen, P. B., Pat, B. K., Gobe, G. C., & Coombes, J. S. (2005). Bcl-2 in endothelial cells is increased by vitamin E and alpha-lipoic acid supplementation but not exercise training. *Journal of Molecular and Cellular Cardiology, 38*, 445–451.

Mendis, E., Kim, M. M., Rajapakse, N., & Kim, S. K. (2007). An in vitro cellular analysis of the radical scavenging efficacy of chitooligosaccharides. *Life Sciences, 80*, 2118–2127.

Morello, F., Perino, A., & Hirsch, E. (2009). Phosphoinositide 3-kinase signalling in the vascular system. *Cardiovascular Research, 82*, 261–271.

Moriue, T., Igarashi, J., Yoneda, K., Nakai, K., Kosaka, H., & Kubota, Y. (2008). Sphingosine 1-phosphate attenuates H_2O_2-induced apoptosis in endothelial cells. *Biochemical and Biophysical Research Communications, 368*, 852–857.

Nam, K. S., Kim, M. K., & Shon, Y. H. (2007). Chemopreventive effect of chitosan oligosaccharide against colon carcinogenesis. *Journal of Microbiology and Biotechnology, 17*, 1546–1549.

Nishimura, K., Nishimura, S., Nishi, N., Saiki, I., Tokura, S., & Azuma, I. (1984). Immunological activity of chitin and its derivatives. *Vaccine, 2*, 93–99.

Parekh, A. B., & Putney, J. W. Jr., (2005). Store-operated calcium channels. *Physiological Reviews, 85*, 757–810.

Shon, Y. H., & Nam, K. S. (2005). Induction of phase II enzymes and inhibition of cytochrome P450 isozymes by chitosanoligosaccharide. *Journal of Microbiology and Biotechnology, 15*, 183–187.

Singha, H. P., Mittala, S., Kaurb, S., Batishb, D. R., & Kohli, R. K. (2009). Chemical composition and antioxidant activity of essential oil from residues of *Artemisia scoparia*. *Food Chemistry, 114*, 642–645.

Tan, S., Sagara, Y., Liu, Y., Maher, P., & Schubert, D. (1998). The regulation of reactive oxygen species production during programmed cell death. *Journal of Cell Biology, 141*, 1423–1432.

Tuo, Q. H., Wang, C., Yan, F. X., & Liao, D. F. (2004). MAPK pathway mediates the protective effects of onychin on oxidative stress-induced apoptosis in ECV304 endothelial cells. *Life Sciences, 76*, 487–497.

Vaux, D. L., Cory, S., & Adams, J. M. (1988). Bcl-2 gene promotes haemopoietic cell survival and cooperates with c-myc to immortalize pre-B cells. *Nature, 335*, 440–442.

Wang, X. (2001). The expanding role of mitochondria in apoptosis. *Genes & Development, 15*, 2922–2933.

Xia, Z., Liu, M., Wu, Y., Sharma, V., Luo, T., Ouyang, J., et al. (2006). N-acetylcysteine attenuates TNF-alpha-induced human vascular endothelial cell apoptosis and restores eNOS expression. *European Journal of Pharmacology, 550*, 134–142.

Xu, J. G., Zhao, X. M., Han, X. W., & Du, Y. G. (2007). Antifungal activity of oligochitosan against phytophthora capsici and other plant pathogenic fungi in vitro. *Pesticide Biochemistry and Physiology, 87*, 220–228.

Xu, Q. S., Dou, J. L., Wei, P., Tan, C. Y., Yun, X. J., Wu, Y. H., et al. (2008a). Chitooligosaccharides induce apoptosis of human hepatocellular carcinoma cells via up-regulation of Bax. *Carbohydrate Polymer, 71*, 509–514.

Xu, S. Z., Zhong, W., Watson, N. M., Dickerson, E., Wake, J. D., Lindow, S. W., et al. (2008b). Fluvastatin reduces oxidative damage in human vascular endothelial cells by upregulating Bcl-2. *Journal of Thrombosis and Haemostasis, 6*, 692–700.

Zhang, H., Du, Y., Yu, X., Mitsutomi, M., & Aiba, S. (1999). Preparation of chitooligosaccharides from chitosan by a complex enzyme. *Carbohydrate Research, 320*, 257–260.

Zhou, S., Yang, Y., Gu, X., & Ding, F. (2008). Chitooligosaccharides protect cultured hippocampal neurons against glutamate-induced neurotoxicity. *Neuroscience Letters, 444*, 270–274.

Zou, W., Yue, P., Khuri, F. R., & Sun, S. Y. (2008). Coupling of endoplasmic reticulum stress to CDDO-Me-induced up-regulation of death receptor 5 via a CHOP-dependent mechanism involving JNK activation. *Cancer Research, 68*, 7484–7492.